Saudi Pharmaceutical Journal 32 (2024) 101984

HOSTED BY

ELSEVIER

Contents lists available at ScienceDirect

Saudi Pharmaceutical Journal

journal homepage: www.sciencedirect.com

Original article

Optimized Ribociclib nanostructured lipid carrier for the amelioration of skin cancer: Inferences from *ex-vivo* skin permeation and dermatokinetic studies

Mohammed F. Aldawsari [a], Mohammad Azhar Kamal [a], Mohamed F. Balaha [b,c], Talha Jawaid [d], Mohammed Jafar [e], Sana Hashmi [f], Majid Ahmad Ganaie [g], Aftab Alam [h,*]

[a] *Department of Pharmaceutics, College of Pharmacy, Prince Sattam Bin Abdulaziz University, Al-kharj 11942, Saudi Arabia*
[b] *Department of Clinical Pharmacy, College of Pharmacy, Prince Sattam Bin Abdulaziz University, Al-kharj 11942, Saudi Arabia*
[c] *Pharmacology Department, Faculty of Medicine, Tanta University, Tanta 31527, Egypt*
[d] *Department of Pharmacology, College of Medicine, Imam Mohammad Ibn Saud Islamic University (IMSIU), Riyadh 13317, Saudi Arabia*
[e] *Department of Pharmaceutics, College of Clinical Pharmacy, Imam Abdulrahman Bin Faisal University, P.O. Box 1982, Dammam 34212, Saudi Arabia*
[f] *Department of Pharmaceutics, Unaizah College of Pharmacy, Qassim University, Unaizah 51911, Saudi Arabia*
[g] *Department of Pharmacology & Toxicology, College of Dentistry and Pharmacy, Buraydah Colleges, 51418 Buraydah, Saudi Arabia*
[h] *Department of Pharmacognosy, College of Pharmacy, Prince Sattam Bin Abdulaziz University, Al-kharj 11942, Saudi Arabia*

ARTICLE INFO

Keywords:
Ribociclib
Nanostructured Lipidic Carriers
BoxBehnken Design
CLSM
Dermatokinetics
Skin cancer

ABSTRACT

Current research focuses on explicitly developing and evaluating nanostructured lipidic carriers (NLCs) for the chemotherapeutic drug Ribociclib (RCB) via the topical route to surmount the inherent bioavailability shortcomings. The absolute oral bioavailability has not been determined, but using a physiologically based pharmacokinetic model it was predicted that 65.8 % of the standard dose of RCB (600 mg) would be absorbed mainly in the small intestine. RCB-NLCs were produced using the solvent evaporation method, and Box-Behnken Design (BBD) was employed to optimize composition. The prepared NLCs had an average PS of 79.29 ± 3.53 nm, PDI of 0.242 ± 0.021, and a %EE of 86.07 ± 3.14. The TEM analysis disclosed the spherical form and non-aggregative nature of the NLCs. The outcomes of an *in-vitro* release investigation presented cumulative drug release of 84.97 ± 3.37 % in 24 h, significantly higher than that from the RCB suspension (RCB-SUS). *Ex-vivo* skin permeation investigations on rodent (Swiss albino mice) revealed that RCB-NLCs have 1.91 times increases in skin permeability comparable to RCB-SUS. Compared to RCB-SUS, RCB-NLCs were able to penetrate deeper into the epidermis membrane than RCB-SUS as per the findings of confocal microscopy. In dermatokinetic study, higher amount of RCB was maintained in both the layers of mice's skin when treated with RCB-NLCs gel comparable to the RCB-SUS gel preparation. The *in-vitro*, *ex-vivo*, CLSM, and dermatokinetics data demonstrated a significant possibility for this novel RCB formulation to be effective against skin cancer.

1. Introduction

The prevalence of skin cancer is rising at a startling speed, and it is now the most prevalent form of cancer in the world (Apalla et al., 2017; Leiter et al., 2014). In the current year, there has been a concerning rise in the count of diagnosed cases across the globe (Leiter et al., 2014; Guy et al., 2015). Based on the most recent statistic report, there are annually recognized about 5.4 million cases of basal cell carcinoma and squamous cell in worldwide while in the United States among 3.3 million patients are diagnosed (Thomas et al., 2021; ASoCO, 2021), highlighting a notable prevalence. In Australia, the annual prevalence of non-melanoma skin cancer (NMSC) exceeds 2,000 cases per 100,000 individuals (Doran et al., 2016). A study from the Australian cancer registry indicates a heightened risk of basal cell carcinoma with increasing age, particularly in those over 80, with an incidence exceeding 12,000 cases per 100,000 persons annually (Perera et al., 2015). Basal cell carcinoma and squamous cell carcinoma (SCC) are frequently identified types of NMSC, with SCC considered the utmost destructive because of its invasive flora and potential for metastasis (Afaq, 2011). Melanoma, however, stands out as an exception. In the realm of skin disorders and

* Corresponding author.
E-mail address: a.alam@psau.edu.sa (A. Alam).

https://doi.org/10.1016/j.jsps.2024.101984
Received 18 November 2023; Accepted 4 February 2024
Available online 10 February 2024

contagion management, the dermal part for medication delivery has emerged as a highly effective administration method, garnering substantial interest in recent times (Cohen, 2010).

Ribociclib (RCB), marketed as Kisqali, is a selective cyclin-dependent kinase inhibitor, authorized by the USFDA in March 2017. Belonging to the class of antineoplastics, RCB hinders cancer spread by targeting cyclin-dependent kinase 4 and 6 (CDK4/6). As a kinase inhibitor it curtails abnormal protein activity, reducing cancer cell proliferation. RCB, with a water solubility of 0.231 mg/mL, is considered weakly soluble but gains protection against inactivation when encapsulated in micelles. Recently designated a breakthrough medicine, RCB received global approval for advanced breast cancer management (Burris, 2018; Infante et al., 2016), promising efficacy with reduced adverse effects and enhanced bioavailability through micelle encapsulation (Fei and Yoosefian, 2021).

Nanostructured lipid carriers (NLCs) represent a promising advancement in topical delivery, offering advantages in encapsulating lipophilic and hydrophobic drugs for improved solubility and stability. With a high surface area and enhanced drug-loading capacity, NLCs allow precise control over drug release kinetics, which is crucial for sustained therapeutic effects. Their nanoscale size facilitates efficient skin penetration, enhancing drug bioavailability at the target site while minimizing systemic exposure and potential side effects. NLCs demonstrate excellent biocompatibility and the ability to incorporate various functional additives, making them versatile for tailored topical formulations. Overall, these attributes position NLCs as a valuable tool for optimizing the effectiveness and well-being of topical delivery systems (Raza et al., 2013; Kumar et al., 2017; Thuy et al., 2022).

Recent past, researchers across the globe have tried various nanosystems, and the majority of them deal with oral delivery and targeting breast cancer; none has attempted to deliver this drug using NLCs by topical route (Sartaj and Annu, 2022; Ahmed et al., 2022; Al-Shdefat et al., 2023; Garaga et al., 2021; Sharma et al., 2022). The rationale behind topical delivery systems is rooted in their ability to provide localized and targeted therapy while minimizing systemic exposure. Topical delivery systems are designed to deliver drugs, medications, or active compounds directly to the skin or mucous membranes, offering several key advantages. RCB belongs to the BCS IV drug category which makes it essential to develop a novel drug delivery system so that NLCs can overcome solubility as well the permeability issue.

2. Materials

Ribociclib (RCB) was procured as a test sample by Hyderabad, India's Alembic Pharmaceuticals Pvt. Ltd. Labrafil, Labrasol, Campritol, Precirol, Gellucire, Stearic acid, Apifil, and Glycerol monostearate (GSM), among other emulsifiers, oils, and lipids, were procured from Gattefosse India Pvt. Ltd. From BASF Mumbai, India, Poloxamer and Cremophor were purchased.Span-20, Span-60, Tween-20 and Tween-80 were acquired from Merck (Germany). From Thomas Baker Chemicals of the New Delhi, India, PEG 400 was purchased. Milli-Q (Millipore, Bedford, MA, USA) provided distilled deionized water that was used. All procedures employed analytical-grade chemicals that were readily available in the lab.

3. Methods

3.1. Selection of solid-liquid lipids

For the selection of lipids, accurately 0.1 g of drug taken in a test tube in which a sufficient quantity of solid lipid (SL) was steadily mixed until they solubilized the drug. The temperature was kept at five degrees Celsius more than the actual melting point (MP) for each SL. The extent to which a clear solution has been observed was chosen. The maximum solubility of the drugs in liquid-lipid were determined by taking liquid lipid (2 ml) in a test tube and adding a sufficient quantity of RCB. The test tube containing the lipid and drug were kept on an automatic shaking at 25 ± 0.5 °C with the stoppers securely in place for 24 h. The supernatant was then centrifuged again, dispersed in methanol, and estimated by UV-spectrophotometer at a wavelength 282 nm (Khan et al., 2016) (See Table 1).

Table 1
Solid lipids with their melting point.

Solid Lipids	Melting Point
Campritol	65–77 °C
Precirol	50–60 °C
Gellucire	42.5–47.5
Stearic Acid	69–71 °C
Apifil	59–70 °C
GSM	55–65 °C

Source: https://www.gattefosse.com and Sigma Aldrich.

3.2. Compatibility of solid-liquid lipids

Different amounts of 5:5, 6:4, 7:3, 8:2, 9:1, 4:6, 3:7, 2:8, and 1:9 were tried and tested for phase separation to find out how well solid–liquid lipids work together. The binary combination was set a higher temperature than MP of each SL, five degrees Celsius higher than the MP of each solid lipid. The blend that didn't show any signs of separating into different phases after 24 h was chosen (Alam et al., 2018).

3.3. Screening of surfactant

100 mgof solid–liquid lipid (Castor Oil, Olive Oil, Sesame Oil, Sunflower Oil, Neem Oil, Lebrafil) was mixed into methylene chloride (3 ml), which was subsequently detached through mild heating. To this organic blend, 10 ml of the corresponding surfactant mixture at a concentration of 5 % w/v were introduced and stirred till 30 min. A one ml sample was extracted and beyond diluted tenfold, after which the % transmittance was estimated at 510 nm by UV spectroscopy (Iqbal et al., 2018; Sartaj and Annu, 2022).

3.4. Formulation of RCB-NLCs

Using the emulsification solvent-evaporation method (Negi et al., 2015; Negi et al., 2014), ribociclib-loaded NLCs (RCB-NLCs) were developed. In a nutshell, the lipidic binary form was made by mixing the drug (10 mg) carefully in the preferred solution of solid liquid (3 %) lipids. Aqueous form was prepared by mixing the surfactant (4 %) in distilled water (20 ml). Ultrasonication with a probe type sonicator (Hielscher, UP-50H, Stahnsdorf, Germany) was then used for 3 minto further reduce the particle size (PS) after the lipid phase was transferred drop-wise with the help of syringe into the aqueous form which being stirred at a constant rotation at magnetic stirrer with 1000 rotation per minute (Remi-Elektrotechnik Ltd., Mumbai, India). The systematic optimization of the formulation composition was performed and has been discussed in the subsequent sections (Alam et al., 2023).

Table 2
BBD independent and dependent factors of the formulation of RCB-NLCs.

Variables	Levels Used		
	Low (−1)	Medium (0)	High (+1)
Independent Variables			
A_1 = Lipid Mixture (%)	2	3	4
A_2 = Surfactant (%)	3	4	5
A_3 = Sonication Time (Min)	2	3	4
Dependent Variables			
B_1 = Particle size (nm)Minimum			
B_2 = EE (%)Maximum			

Table 3
Obtained value in BBD technique for the preparation of RCB-NLCs and results of regression study for value B_1 andB_2.

Runs	Space Type	Independent Variables		Dependent Variables		
		A_1	A_2	A_3	B_1	B_2
1	IBFact	4	4	2	122.73 ± 3.54	82.04 ± 1.84
2	IBFact	3	5	4	109.37 ± 4.32	76.82 ± 2.32
3	IBFact	2	5	3	106.56 ± 3.12	76.97 ± 2.18
4	IBFact	3	3	4	114.68 ± 5.33	80.33 ± 1.95
5	IBFact	4	3	3	122.32 ± 5.04	82.82 ± 2.09
6	Center	3	4	3	80.24 ± 2.47	85.68 ± 2.15
7	IBFact	2	4	4	113.84 ± 2.06	79.98 ± 1.75
8	IBFact	4	4	4	117.98 ± 2.86	81.08 ± 2.87
9	Center	3	4	3	81.01 ± 2.76	85.51 ± 2.13
10	Center	3	4	3	79.29 ± 2.32	86.07 ± 2.58
11	IBFact	2	4	2	112.68 ± 3.17	79.85 ± 1.48
12	IBFact	2	3	3	110.25 ± 2.27	79.88 ± 1.67
13	Center	3	4	3	80.42 ± 2.66	85.85 ± 2.11
14	IBFact	4	5	3	115.54 ± 4.02	80.49 ± 2.48
15	Center	3	4	3	79.98 ± 2.49	85.62 ± 2.69
16	IBFact	3	3	2	118.97 ± 4.28	80.01 ± 1.85
17	IBFact	3	5	2	113.48 ± 3.88	79.04 ± 1.35

Quadratic model	R^2	*Adjusted* R^2	*Predicted* R^2	*SD*	*C.V. %*
Response (Y_1)	0.9977	0.9948	0.9683	1.22	1.16
Response (Y_2)	0.9891	0.9751	0.8441	0.49	0.60

A_1 = Lipid Mixture (%), A_2 = Surfactant (%), A_3 = Sonication Time, B_1 = PS (nm), B_2 = EE (%).

3.5. Experimental design for optimization of RCB-NLCs

Using software DesignExpert version13.0, the selected three variables (lipid, surfactant mixture, and sonication time) were optimized based on three variables [PS, and EE-(Entrapment Efficiency)] for the preparation of NLCs with the anticipated physicochemical properties. The optimization research used a system where the independent and dependent factors each had their own unique set of codes. Dependent levels were selected as follows: "B_1'' for PS (nm), and " B_2'' for EE (%), while independent levels were designated as follows: "A_1'' for lipid mixture (2–4 %), "A_2'' for surfactant mixture (3–5 %), and "A_3'' for sonication time (2–4 min). Table 2 summarizes the aforementioned parameters and their values. Box-Behnken designs are used to generate higher order response surfaces using fewer required runs than a normal factorial technique. The BBD offers 17 permutations for use in creating NLCs to develop a proper understanding within the design space (Gupta et al., 2020, Sartaj and Annu, 2022).The center points are important for Box-Behnken Design as this design is devoid of corner points and the center points improve the predictability. The link between the independent and dependent variables was further evaluated by generating polynomial equations and various response graphs using the chosen model (Alam et al., 2023;Rizwanullah et al., 2021).The design's validation involved the random selection of three compositions recommended by the software, including the optimized version.(Table 3).

3.6. Evaluation parameters for the optimization of RCB-NLCs

3.6.1. PS, polydispersity index (PDI) and Surface-Charge

The Zeta-sizer Nano ZS from Malvern, United Kingdom was the instrument employed for the determination of PS distribution and particle distribution index based on the dynamic light scattering. The same instrument employed for the estimation of the zeta potential (the representative of surface charge) and done in triplicate (Khan et al., 2019; González-Mira et al., 2011).

3.6.2. %EE and drug loading (%DL)

The ultracentrifugation method was utilized in order to provide an indirect determination of the RCB-NLCs' drug EE and DL percentages. In a nutshell, the preparations were put into a centrifuged tube and put through a high speed centrifugation using a Sigma 3 K30 from Sigma Laborzentrifugen GmbH in Osterode am Harz, Germany. The centrifugation was performed at 15,000 revolutions per minute for fifteen minutes or Relative Centrifugal Force is 12,577 xg. Following that, the supernatant was gathered, the required amount of methanol was added to dilute it and filtered by 0.2 μm membrane filter. After that, UV spectroscopy was used to provide a quantitative reading on the amount of unencapsulated drugs (Soni et al., 2018). In the end, the below equations were utilized to find out the %EE and %DL values.

$$\%\,EE = \frac{Totaldrug - Unencapsulateddrug}{Totaldrug} \times 100$$

$$\%\,DL = \frac{Totaldrug - Unencapsulateddrug}{TotalweightofNLCs} \times 100$$

3.7. TEM

The size of the optimized RCB-NLCs preparation were determined by transmission-electron-microscopy (TEM). The sample of RCB-NLCs was prepared for analysis by first being diluted with distilled water by 10 times and then being plated onto a copper grid with a pore size of 400 which covered with carbon film. Next, phosphotungstic acid (1 %) solution was applied as a negative stain to the copper-grid prepared. The solution that was placed on top of the copper grid was allowable to dry out in the air. After that, the sample that had been dried was sent through the TEM. Bright field imaging was utilized to establish the size and form of the NLCs by employing a configuration that involved increased magnification in conjunction with diffraction modes contained within the device (Luo et al., 2011).

3.8. Evaluation of in-vitroRCBrelease

The dialysis membrane (DM) having molecular weight of 12–14 kDawas employedforthe evaluation of the *in-vitro* drug release. A volume of three milliliters of the ribociclib suspensions (RCB-SUS) and RCB-NLCs (1 mg/ml) were added to the DM separately. The DM was then subjected to an incubation process in buffer medium consisting of PBS with a pH of 6.8 and 5.5. The samples were evaluated while being stirred continuously at 37 degrees Celsius. 1 ml of the buffer solution was withdrawn at each time-point (1, 2, 3, 4, 6, 12, 18, and 24 h) and same volume of freshly prepared buffer solution was added into it. After that, the amount of drug that was present was determined at each time point with the use of a UV spectrophotometer set at 282 nm, and then*in-vitro* release curve was drawn (Sartaj and Annu, 2022).

3.9. DPPH assay

The radical DPPH is called to be stable and produces a very dark violet color when its extra electron or hydrogen radical is de-localized. The RCB-NLCs were comparable to both a pure RCB suspension and an ascorbic acid reference standard in order to assess their antioxidant potential. Based on how successfully DPPH neutralized free radicals while the temperature was held at room temperature, an estimate was made. The resulting methanolic solutions included quantities of all three substances varying from 1 to 80 μg/mL. Then, a methanolic solution of DPPH (1 ml) was added to one milliliter of all sample. The mixture was scanned at 515 nm with 95 % methanol acting as a blank after 30 min (Moolakkadath et al., 2018; Gupta et al., 2020). The proportion of DPPH inhibition obtained was evaluatedbybelow equation:

$$\%\,InibitionofDPPHRadical = \frac{Ac - As}{Ac} \times 100$$

where, Ac and As are control and sample absorbance, respectively.

3.10. Preparation of RCB-NLCsGel and RCB-SUS gel

Due to their inadequate viscosity, RCB-NLCs are difficult to apply to the skin. As a result, the improved RCB-NLCs were turned into gels by adding the Carbomer 940 (1 % w/w) acts as gelling agent while stirring continuously and keeping the magnetic stirrer set at 1000 rpm until the Carbomer was completely disseminated. The resultant combination was then allowed to expand for an additional day before being neutralized with a 0.05 % w/w TEA (triethanolamine) additionand transformed into RCB-NLC gel. The RCB-SUS gel was made using a similar process (Gupta et al., 2020; Iqubal et al., 2021).

3.11. Evaluation of RCB-NLCs gel

3.11.1. Physical Appearance, pH, and drug content

Visual inspection was done of the produced gels' physical attributes and homogeneity. At room temperature, the pH of the gel formulation have being evaluated by a pH meter (Mettler Toledo MP 220, Greifensee, Switzerland). To evaluate the homogeneity of pharmaceuticals, present in the produced gels, the drug content was determined. 1000 mg of gel was mixed in methanol (10 ml), filter by 0.2 μm membrane filter, properly diluted, and then exposed to UV Spectroscopy to determine the RCB content (Shah et al., 2007).

3.11.2. Viscosity and spreadability

Viscometer was utilized to assess the gel viscosity of the RCB-NLCs. At ambient temperature, the device was run at 100 rotational speed per minute for 160 s (Aziz et al., 2017). The assessment of spreadability was carried out by marking a 1 cm diameter on a tissue plate and applying 500 mg of gel. Another platter was set on the upper of the first, and a 500 gm load was utilized to the upper plate for 5 min. Expansion in diameter was measured to determine the gel spreadability as a function of weight. (Harde et al., 2015).

3.11.3. Texture analysis of gel

A texture analyser ("TA.XT Plus Texture analyzer, Stable Micro-Systems Ltd., Surrey, UK") was employed for measurement of texture. The graph obtained after the analysis which provided information on parameters like hardness, cohesiveness, consistency and the viscosity index of the gel.

3.11.4. Skin permeation study by ex-vivo

Ex-vivo skin penetration tests were done on RCB from different mixtures using full-thickness, hairless abdominal skin from mice that had been cut off. The skin section wasset on Franz diffusion cells with a surface area of 0.785 cm^2 and a receptor capacity of 10 ml. The dermal part of the skin was subjected to the receptor solution (methanol: PBS (pH 6.8) in 30:70 v/v ratio), and the stratum corneum stayed in contact with the contents of the donor part. Various mixtures (RCB-NLCs gel and RCB-SUS gel) were put in the donor section so that one could evenly cover the whole skin surface at temperature 37.0 ± 1.0 °C. Samples were taken at different times up to 24 h, and the RCB level was measured with UV spectroscopy (El-Housiny et al., 2018).

3.12. Confocal laser scanning microscopy

CLSM method was used to estimate the depth of penetration of the produced NLCs. Using CLSM, we measured the amount of rhodamine-B dye absorbed by mouse skin after being placed onto the improved RCB-NLCs formulation and assessed the data to those obtained using a control (rhodamine B hydro-ethanolic solution). For the CLSM analysis, rhodamine B loaded RCB-NLCs gel and rhodamine B hydro-ethanolic solution were subjected to an 8-hour*ex-vivo* skin penetration investigation using "Franz diffusion cells" made from the skin of mice. Samples of skin were generated on glass slides, seen under a CLS microscope, and probe dye permeation was determined (Gupta et al., 2020).

3.13. Dermatokinetic estimation

The optimal RCB-NLCs formulation was established for a dermatokinetic research in the epidermis and dermis over multiple time points. The drug's removal or breakdown by skin enzymes must be estimated, as must its retention in various skin layers. Use of a maximum strength of the medicine to the skin results in the highest possible levels of the drug being absorbed through the skin. The kinetic appearance of drug which are taken topical are affected by these factors. RCB-NLCs loaded gel and RCB-SUS loaded gel were tested for dermatokinetics at set time points (0, 1, 2, 4, 6, and 8 h) on freshly skinned mice. At the end of the study, the skins were cleaned in saline buffer to get rid of any leftover medication that hadn't been absorbed, and then the epidermis and dermis were carefully dissected. Acetonitrile was employed to remove the medication from the scraped-apart skin layers. The solution from which the medication was isolated was centrifuged, and the resulting supernatant was saved. UV Spectroscopy was used to evaluate the solution after filtering with 0.2 μm nylon filter. Dermatokinetic characteristics were assessed by plotting the estimated RCB strength in the skin of epidermis and dermis. T_{max}, C_{max}, and $AUC_{0\text{-}8h}$ were calculated using the non-compartmental pharmacokinetic model (Thotakura et al., 2017; Nair et al., 2013).

3.14. Stability study

The RCB-NLCs gel were kept in sealed containers and their physical stability during storage was evaluated in accordance with ICH Q1A (R2) requirements (FDA, 2003). Determining in detail to know about the content strength alterations throughout time in response to change in temperature and humidity is the primary goal of stability analysis. The RCB-NLCs formulation was subjected to six months of stability study in a stability chamber, according the ICH's recommendations. The NLCs were stored at 25 °C, 32 °C and 40 °C with range ± 2 °C and 60 % RH, 60 % RH and 75 % RH with range ± 5 % RH respectively, in stability chambers. Samples were taken at the beginning, after one month, two months, three months, and six months to check for alterations in colour, odor, homogeneity, pH, and viscosity (Waghule et al., 2021).

3.15. In vivo efficacy studies

3.15.1. Animal

The Standing Committee of Bioethics Research at Prince Sattam bin Abdulaziz University in Al-Kharj, Saudi Arabia (SCBR-020–2023) approved the use of animals as per the disclosed protocol. In the pharmacodynamic investigations, Swiss albino mice with a weight range of 22–26 g were employed.

3.15.2. Drug administration

The mice were accommodated in a well-ventilated environment at a temperature of 25 ± 2 °C, following a 12hrs light and dark cycle.

Mice in the study were provided with a pellet-diet and had accessible to drinking water without restrictions. The study was allocated into 4 groups, each consisting of three animals.

Group-I: Selected as the control group and with no treatment.

Group-II: Selected as the carcinogen group.

Group-III: Received treatment with a 5-Fu (Flonida cream, Shalak Pharmaceuticals), which was utilized to protect the lesions twice daily for a duration of six weeks.

Group-IV: Was given with a 1 % RCB-NLCs gel, which was also applied to cover the lesions twice daily for 6 weeks.

The front part of the mice skin was removed using electric-clipper, and a hair removing cream (Veet, Reckitt) was applied minimum 2 days before the treatment (Chaudhary et al., 2009). Skin tumorigenesis was introduced by topically applying 7,12-dimethylbenz(a) anthracene (DMBA) at a 72-hour interval, at a strength of 0.05 gm/kg body weight in acetone (100 ml/mouse). This was followed by the application of

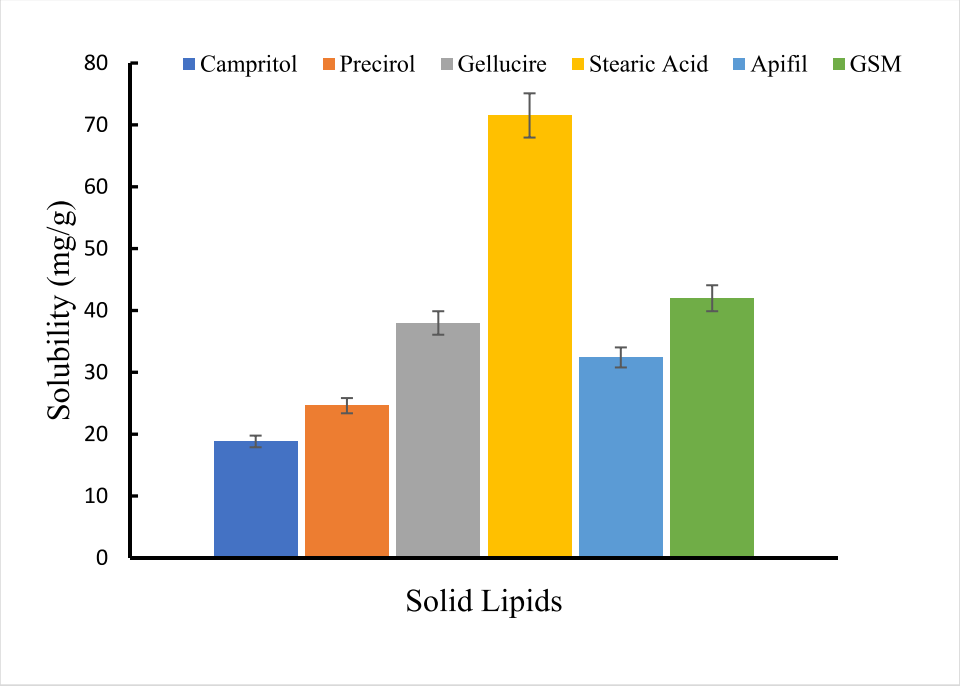

Fig. 1. Solubility of RCB in different solid-lipids.

croton oil (1 % w/v) in acetone (100 ml/mouse) administered two times a week up to the 9th week, beginning from day 8 after the initial DMBA application.(Hennings et al., 1981;Das et al., 2005; Malik et al., 2023).

3.16. Characteristics of efficacy

3.16.1. Visual appearance

Following the application of the commercial preparation and the optimized RCB-NLCs gel, the mice were intimately examined for alterations in skin tumors. Visual assessments of the tumor sites were conducted at the end of the 2nd, 4th, and 6th weeks after the individual treatment. The skin scoring was based on tumor shape and size, with a scale of 0 indicating no change, 1 denoting mild, 2 representing moderate, and 3 indicating the highest tumor size. The reported grade was determined as an average for the entire group (Xing et al., 2021; Batool et al., 2023).

3.17. Biochemical analysis

3.17.1. Preparation of tissue homogenate

As the treatment completed, the animals were humanely euthanized. A 1 cm^2 portion of skin at the tumor spot was surgically removed and rinsed with a saline solution. Subsequently, the excised tissue was fragmented into minute pieces and homogenized in a solution comprising 3 volumes of PBS with a pH of 7.4 at a temperature of 4 °C. Following homogenization, the mixture underwent centrifugation at 12,000 rpm for 20 min at the same 4 °C temperature. The resultant lower part was taken and employed for subsequent biochemical analysis.

3.17.2. Lipid peroxidation estimation

Lipid peroxidation assessment involved measuring thiobarbituric acid reactive substances in the tissues, following the protocols outlined by Yagi (1987) and Ohkawa et al. (1979). For this analysis, 0.1 ml of the supernatant was placed in a glass tube. Added 0.1 ml of TrisHCl buffer, $FeSO_4$, and ascorbic acid, and the volume makeup to one ml using double-distilled water. The resulting combination was incubated at 37.0℃ for 15 min. After incubation, added 1 ml of 10 % TCA and 2 ml of 0.375 % TBA reagent to the reaction. The glass tubes were shielded with aluminum foil and placed in a shaking water-bath for half an hour at 80℃. Following incubation, the tubes were removed and immersed in ice cold water for an additional 30 min. Subsequently, the tubes were centrifugation at 3000 rpm for 15 min, and the absorbance of the filtrate was measured at 532 nm reference to blank. The concentration of malondialdehyde was determined by a specific equation:

$$\text{Concentration} : A \times (V/E) \times P$$

where A: Absorbance, V: Volume, E: Extinction coefficient ($1.56 \times 10^{-6} M^{-1} cm^{-1}$), P: Protein contents of the tissue estimatedinmg of proteins per gram of tissue.

3.17.3. Skin irritation study

Swiss albino mice (male) weighing 25–30 g were employed in a skin irritation test. Two groups, each consisting of three mice, were utilized for the experiment. The mice were housed in controlled laboratory conditions at temperature of 25.0 ± 1.0℃ and RH 55 ± 5 %. Polypropylene cages, accommodating six mice per cage, were used, and the mice had unrestricted access to laboratory facilities and water throughout the study.

The main purpose of this analysis was to assess the formulation's skin suitability. A single application of the preparation was administered to the left side ear of the mice, while the right-side ear was left untreated as a control. The occurrence of erythema, which is indicative of cutaneous vascular dilatation, was supervised daily over a 7-day period, following the methodology detailed by Uttley and Van Abbe (1973). Each day, an average score was calculated using the Uttley & Van Abbe (1973) scoring scale, and the collected data were subsequently interpreted:

- Scores from 0 to 9: Probably not noticeably irritant to human skin.
- -Scores from 10 to 15: May be slightly irritant to some users.
- Scores over 15: Likely to be significantly irritant to some users, potentially leading to unacceptable levels of complaints.

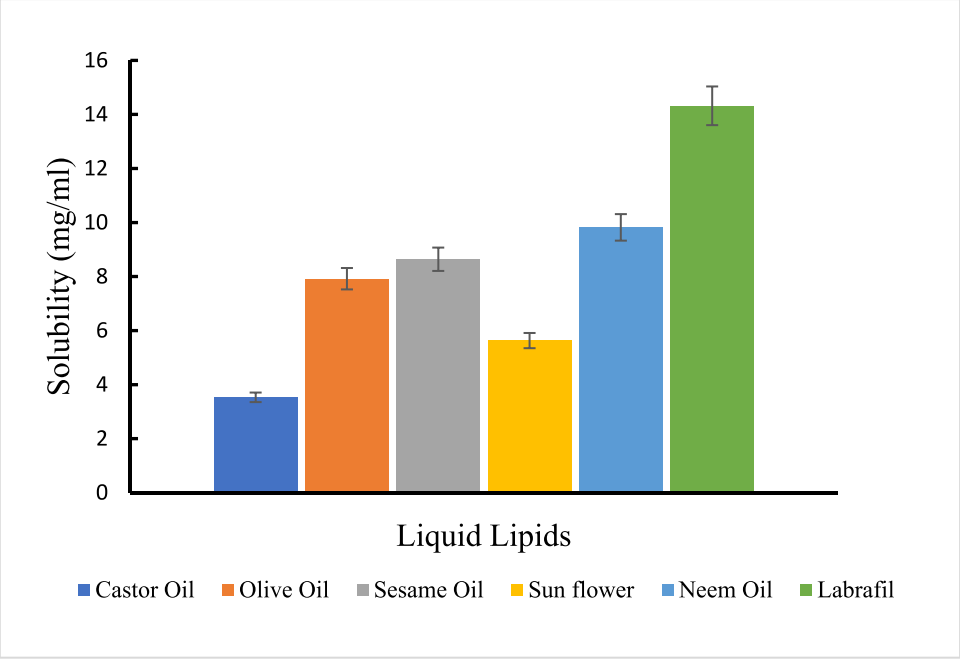

Fig. 2. Solubility of RCB in different liquid-lipids.

4. Results

4.1. Selection of solid-liquid Lipids

The maximal solubility of the drugs in each ingredient was taken into consideration when choosing different necessary elements, such as lipids, for the manufacture of NLCs. Several lipids were used to test the solubility of RCB, and the findings are detailed in Figs. 1 and 2.

As per the data, Stearic acid was chosen because solid lipids have demonstrated significant levels of RCB solubility, and it was expected that each solid lipid's carboxylic acid group-containing structure would promote RCB solubility. In additional, longer triglycerides have demonstrated greater solubility than medium chain ones because more medicines are bound to them. Labrafil also shown high solubility for the same causes. Each lipid's solubility properties directly reflect the effectiveness of encapsulation. As a result, the high encapsulation effectiveness of the NLCs preparation is also reliable for the drug's high solubility in lipids (Nabi et al., 2020).

4.2. Compatibility of solid-liquid lipids

The compatibility of the solid–liquid lipid in various binary mixing ratios was established. For the investigation, the binary combination was set temperature that was highest than the MP of each solid lipid (5 °C higher). Binary mixture with an observed ratio of 7:3 did not phase separate until 24 h of observation, as indicated in Table 4. So, this ratio was chosen for further exploration.

Table 4
Screening of binary solid–liquid lipid mixture ratio.

Solid Lipid	Liquid Lipid	Ratio	Inference
Stearic acid	Labrafil	5:5	Phase separation
		6:4	No-Phase separation
		7:3	No-Phase separation
		8:2	No-Phase separation
		9:1	Phase separation
		4:6	Phase separation
		3:7	Phase separation
		2:8	Phase separation
		1:9	Phase separation

Table 5
% Transmittance of binary lipid mixture by different surfactants.

Name of surfactant	% Transmittance
Tween 80	74.86 ± 7.53
PEG 400	81.65 ± 5.31
Labrasol	86.31 ± 7.12
Tween 20	56.73 ± 4.63
Cremophor	93.42 ± 9.34
Span 20	79.43 ± 5.23
Span 60	58.75 ± 6.74
Poloxamer	89.12 ± 8.43

4.3. Screening of surfactant

The emulsification properties of the surfactants Cremophor, PEG 400, Tween-20, Tween-80, Span- 20, Span-60, Labrasol, and Poloxamer were assessed. Table 5 provides an example of the screening's outcome. The increased physical stability of lipid nanoparticles and reduced particle size of binary mixture lipids result from the better emulsification characteristic, which also prevents nanoparticle aggregation, which results in higher transmittance (Teng et al., 2019). Isradipine NLCs were developed by Alam and colleagues. They discussed the criterion for choosing a surfactant based on transmittance percentage in their research (Alam et al., 2018). This was done using a UV spectroscopic technique at 510 nm.

4.4. Formulation and optimization of RCB-NLCs by BBD

In order to prepare the RCB-NLCs, the emulsification solvent evaporation approach was effectively used. This method of creating NLCs is quick and effective, and it can result in nanoscale particles. BBD suggested 17 experimental compositions, as shown in Table 3, to optimize the RCB-NLCs. Utilizing analysis of variance (ANOVA), the impact of independent variables (A_1, A_2, and A_3) on dependent variables (B_1, B_2, and B_3) was measured and statistically assessed. To find the model with the greatest adjusted and projected R^2, the regression analysis results for each of the three dependent components were individually fitted into several models. The data were recorded in Table 3. The data exhibited a strong match between the recommended quadratic models and the data,

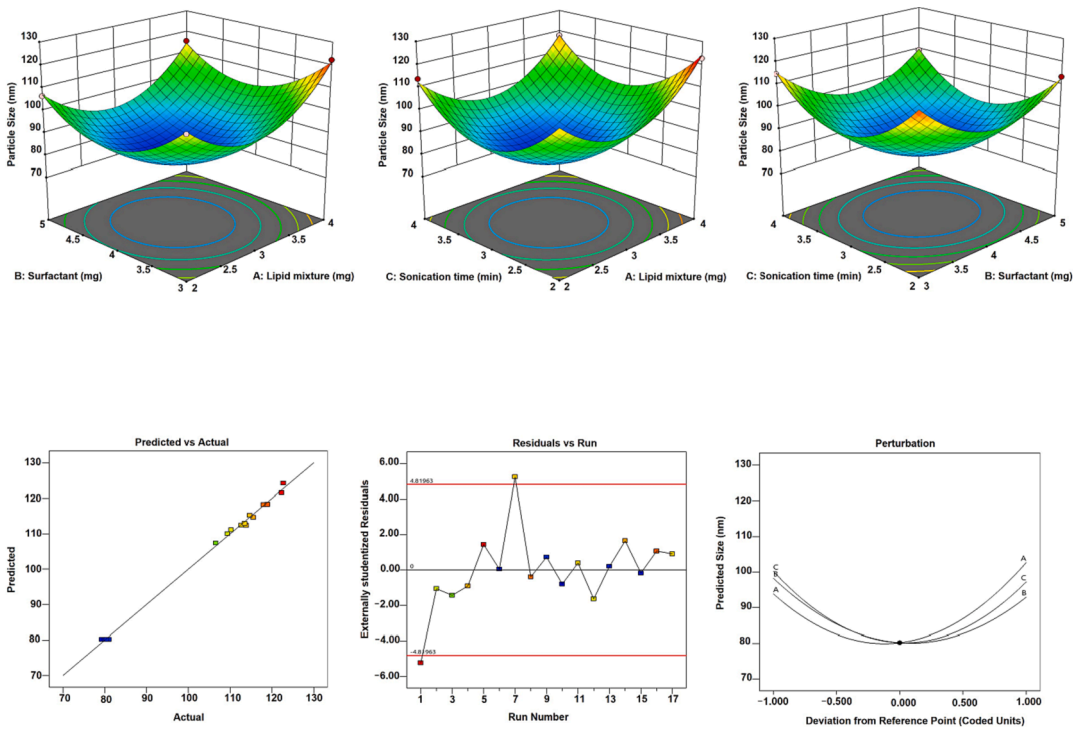

Fig. 3. Representation of (A) 3D surface plot, (B) Predicted level vs Actual level, (C) perturbation graph t, (D) residual level vs. run graph on the effect of independent levels on particle size.

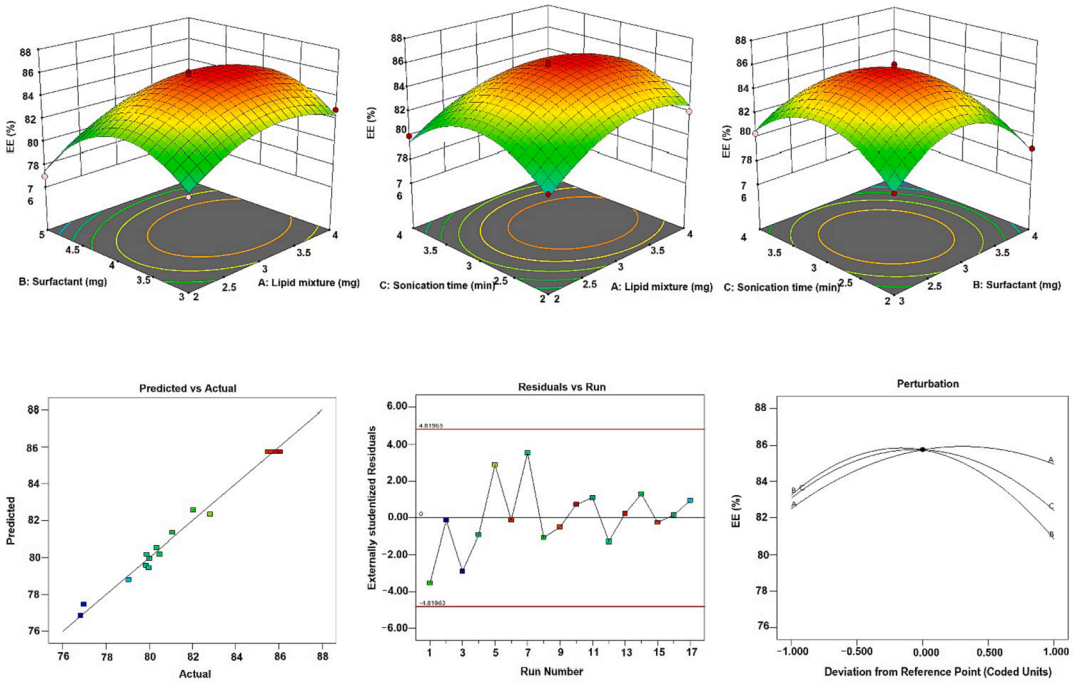

Fig. 4. Representation of (A) 3D surface plot, (B) Predicted level vs Actual level, (C) perturbation graph, (D) residual level vs. run graph on the impact of independent levels on EE.

with model terms being highly significantly for each of the three dependent components. Based on the results quadratic polynomial model was utilized in these equations, The "Predicted $R^{2\prime\prime}$ values for each of the three dependent levels were relatively near to the matching "Adjusted $R^{2\prime\prime}$ values. Figs. 3-4 displays the 3D surface graph, predicted response vs. actual graph, perturbation graph, and residual vs. run graphs that were produced for each dependent component.

4.5. *Effect on particle size (B_1)*

When developing nano-formulations, one of the most crucial quality characteristics is the PS since it impacts both the rate of permeation and the amount of medicine that is accumulated inside the skin. A preparations particle size must be under 200 nm for it to be properly transported to the skin (Iqbal et al., 2018). The PS distribution of the RCB-

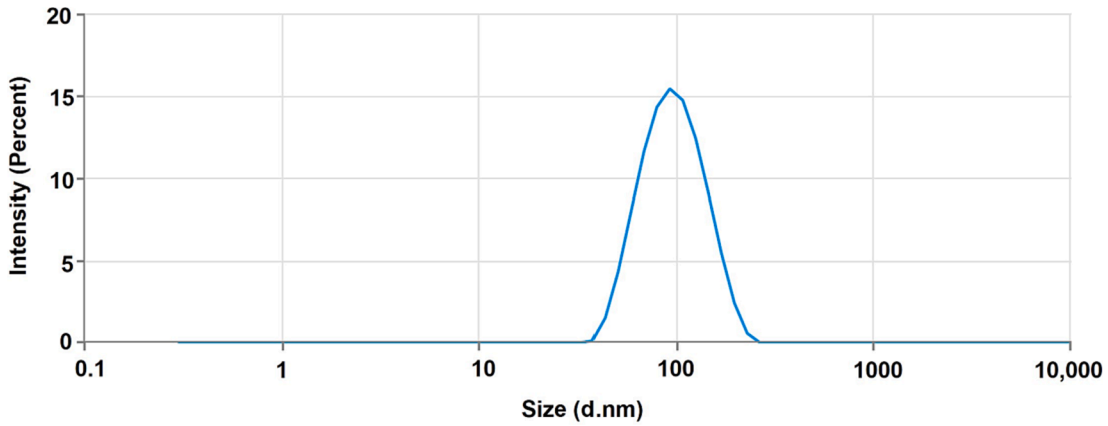

Fig. 5. Average particle size of the RCB-NLCs using zetasizer.

NLCs observed from the several experimental runs suggested by BBD is illustrated in Table 3. The average PS ranged between 79.29 and 122.73 nm when several investigational values were considered. The calculated polynomial equation has the following expression

$$B_1 = +80.19 + 4.41A_1 - 2.66A_2 - 1.50A_3 - 0.7725A_1A_2 - 1.48A_1A_3 + 0.0450A_2A_3 + 18.08A_1^2 + 15.40A_2^2 + 18.54A_3^2$$

The PS distribution of the RCB-NLCs exhibits variation in response to changes in the values of independent components, as described by the quadratic Equation (1) and illustrated in Fig. 3. The overall relationship between the strength of the lipid mixture and PS is positive, indicating that as the lipid fraction increases, the NLCs' particle size significantly increases. This increase in PS is attributed to the insufficient surfactant amount, which fails to adequately emulsify the growing lipid content within the aqueous phase of the preparation (Subedi et al., 2009). Conversely, an upsurge in surfactant amount leads to a decrease in interfacial tension between the lipid form and aqueous form, resulting in the preparation of smaller particles, indicating a negative effect of surfactants on the NLCs' particle size (Shtay et al., 2018). Moreover, a maximum strength of surfactants, up to a threshold micelle strength, effectively stabilizes the NLCs by creating a steric barrier on their surface, preventing smaller NLCs from aggregating into larger ones (Singh et al., 2019).

As the sonication period increases, more sonication energy is imparted to the nano-particle dispersion due to the generation of significant shear forces during cavitation. This breakdown of bigger particles into minor, mono-dispersed droplets result in a reduced PS distribution of the NLCs (Alam et al., 2018).

4.6. *Effect on entrapment efficiencies (B_2)*

As per the requirement of distributing the therapeutic effective dosage of the medication contained in the NLCs, EE is a critical component in the preparation of NLCs. The %EE of the RCB-NLCs observed from the different investigational run suggested by BBD are shown in Table 3. After taking into account several testing run, it was discovered that the RCB's average %EE varied from 76.82 to 86.07 %. The following is how the computed polynomial equation for the RCB's % EE is stated:

$$B_1 = +85.75 + 1.22A_1 - 1.21A_2 - 0.3413A_3 + 0.1450A_1A_2 - 0.2725A_1A_3 + 0.6350A_2A_3 + 2.01A_1^2 - 3.70A_2^2 - 3.00A_3^2$$

The %EE of RCB-NLCs varied after the values of independent components were modified, in accordance with the coded quadratic above Equation and the different graphs displayed in Fig. 4. As additional room was made available for the RCB solubilization in the lipid matrix of the NLCs, an increase in the lipid mixture's amount followed an upsurge in the formulation %EE. Additionally, by converting the lipid matrix into an irregular lattice, the inclusion of a liquid lipid improved the drug EE (Alhalmi et al., 2022). Other side, the %EE of the NLCs is negatively impacted by the surfactant content. Overly high surfactant concentrations result in the production of mixed micelles, which contain both medicines and surfactants and co-exist with lipid nano-particles to lessen drug entrapment (Alam et al., 2018). Another explanation is that when surfactant concentration rises, drug diffuse from the lipid matrix to the exterior phase and are subsequently less likely to become trapped in NLCs (Singh et al., 2019).The % EE of the RCB-NLCs decreased as the

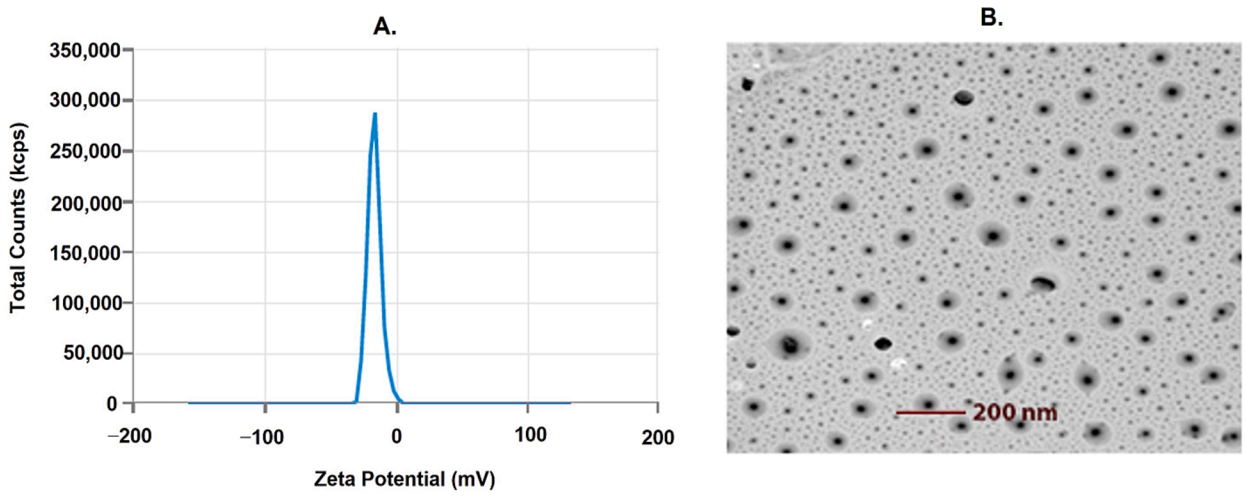

Fig. 6. (A) Zeta Potential, (B) TEM of optimized RCB-NLCs preparation.

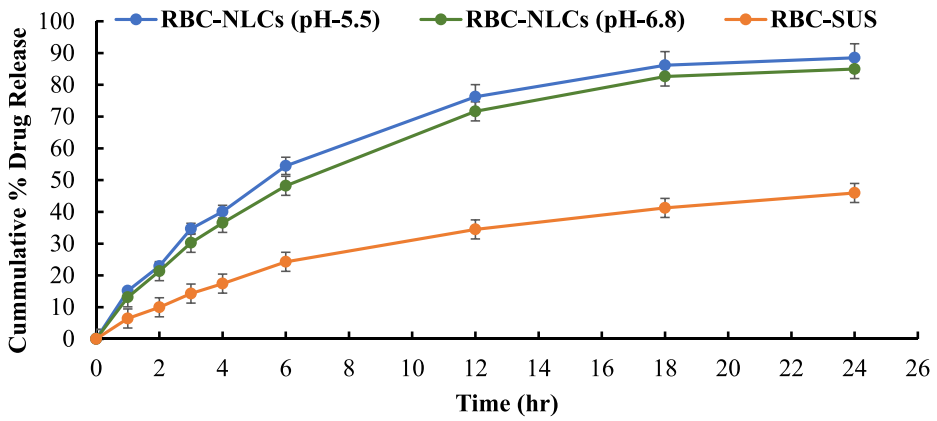

Fig. 7. *In-vitro*RCB release from RCB-NLCs and RCB-SUS at pH 5.5 and 6.8.

sonication period was extended. Longer sonication periods may have provided more sonication energy, which may have caused NLCs to rupture and cause drug outflow as a result (Ghazwani et al., 2023).

4.7. Selection of optimized preparation composition

The optimization method BBD of Design Expert was used for the optimization of formulation composition.On the basis of predetermined objectives, such as small PS and high % EE, the optimal formulation composition was chosen. Dependent on the useful PS, and % EE goal, the numerical optimization component of BBD recommended condition for the preparation of RCB-NLCs as 3.25 % lipidmixture, 4.85 % surfactants mixture, and 2.08 min sonication time, with corresponding predicted values for PS of 89.23 nm and%EE of 84.48 for RCB, respectively. The optimized NLCs were created using the right combination of component and process parameters. The RCB-NLCs, actual experimental PS and % EE values were discovered to be 79.29 nm and 86.07 % for RCB, respectively showing a higher degree of prognosis and predictability (Alam et al., 2023).The pure error for PS was 1.58 and for EE is 0.1917 sum of squares and having desirability function 1.0.

4.8. Characterization parameters of optimized RCB-NLCs

4.8.1. PS and PDI

Nanovesicles smaller than 300 nm can penetrate deeper into the skin layers to a certain degree. Specifically, those with a size less than 100 nm demonstrate optimal delivery to both the viable dermal and epidermal layers (Danaei et al., 2018).The PS and PDI were observed at 79.29 ± 3.53 nm and 0.242 ± 0.021, respectively as displayed in Fig. 5. Lower PS suggests good biological acceptability and above systemic circular time. The minimum PDI value denotes the uniformly of PS distribution (Varshosaz et al., 2018).

4.8.2. Surface charge determination and morphology

According to Fig. 6A, the zeta potential of RCB-NLCs was measured to be −15.40 ± 0.87 mV. The nano-formulation stability is shown by the zeta potential. Here, the formulation's lipids and nonionic surfactant could be given credit for the negative charge, which resulted in a smaller magnitude of nanoparticles without having aggregation, demonstrating the stability of the RCB-NLC. Fig. 6B shows the TEM images of the developed nano-dispersion and the particles were observed to be spherical in shape and devoid of any visual sign of aggregation.

4.8.3. %EE and %DL

The %EE of RCB in RCB-NLCs was discovered to be 86.07 ± 3.14 %, demonstrating that optimized RCB-NLCs demonstrated increased drug entrapment at the optimal lipid matrix concentration. The greater drug entrapment effectiveness in NLCs, which results in a larger drug payload capacity, may be attributed to the lipophilicity of the medicines and the defective crystal shape of NLCs (Jenning et al., 2000). The optimized RCB-NLCs were found to have an RCB%DL of 14.5 ± 0.31.

4.8.4. Evaluation of in-vitro RCB release

Over the course of 24 h, the cumulative percentage discharges of RCB

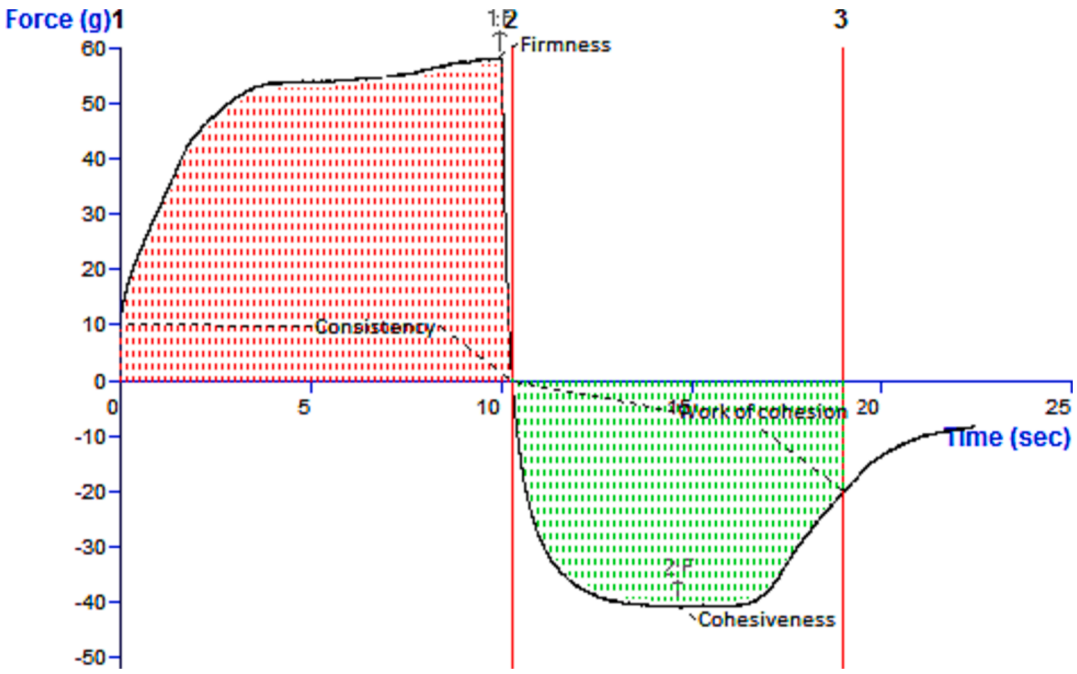

Fig. 8. Texture analyzer image of RCB-NLCs gel.

from RCB-NLCs and RCB-SUS were assessed *in-vitro* by an activated dialysis membrane bag. Fig. 7 displays the respective release patterns for RCB-SUS and RCB-NLC formulations based on the mean % of the cumulative drug permeates that were assessed at pH 6.8 and 5.5. With an early burst delivery pursued by a somewhat continuous drug release, RCB-NLCs showed a biphasic release pattern, at pH 6.8 with 84.97 ± 3.37 % and pH 5.5 with 88.50 ± 3.02 % of the drug released at 24 h. As per the data observed there was almost similar release shown at pH 6.8 and 5.5.A portion of the RCB may have precipitated from the surface lipid matrix or may have been adsorbed onto the NLC's surface, which would have led to the first burst release. However, the prolonged drug release from RCB-NLCs shows that RCB were diffused out into the release medium from the lipid-matrix core of the NLCs. On the other hand, because RCBs are lipophilic, the RCB-SUS released RCBs slowly, only 45.95 ± 2.14 % in 24 h. Analogous reports of slower release of drug from the suspension have been previously discussed (Sartaj and Annu, 2022).

The Korsmeyer-Peppas model was chosen after mounting the *in-vitro* release outcomes into several release kinetic models; it had a higher R2 value of 0.9782 for RCB from RCB-NLCs. It was discovered that RCB had release exponents (n) from RCB-NLCs was 0.3 which less than 0.5, which is suggestive of a Fickian diffusional procedure for their release.

4.8.5. DPPH assay

By monitoring the color shift from purple to yellow, which was quantified at an absorbance of 515 nm, the capacity of DPPH to decrease was ascertained. The results show that the RCB-NLCs had a considerable influence on the free radical scavenging procedure. It is often better to concentrate on increasing their antioxidant capacity while trying to improve the efficacy of nano-formulations in the management of neurological brain disorders. The fact that the combined effects of RCB were shown to increase the antioxidant activity of the RCB-NLCs is proof that these substances are potent antioxidants. RCB-NLCs were shown to have an antioxidant activity of 81.26 %, while ascorbic acid had an antioxidant activity of 94.04 % (Gupta et al., 2020).

4.9. Formulation and characterization of RCB-NLCs gel and RCB-SUS gel

4.9.1. Physical appearance, pH, and drug content

RCB-NLCs gel had a light yellowish color, was spread evenly, and

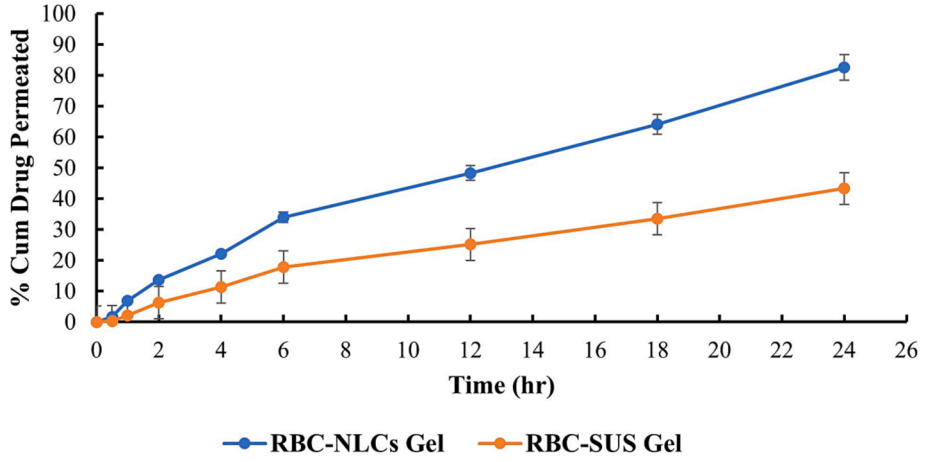

Fig. 9. Ex vivo graphs show cumulative amount of RCB permeated through skin using RCB-NLCs Gel and RCB-SUS Gel.

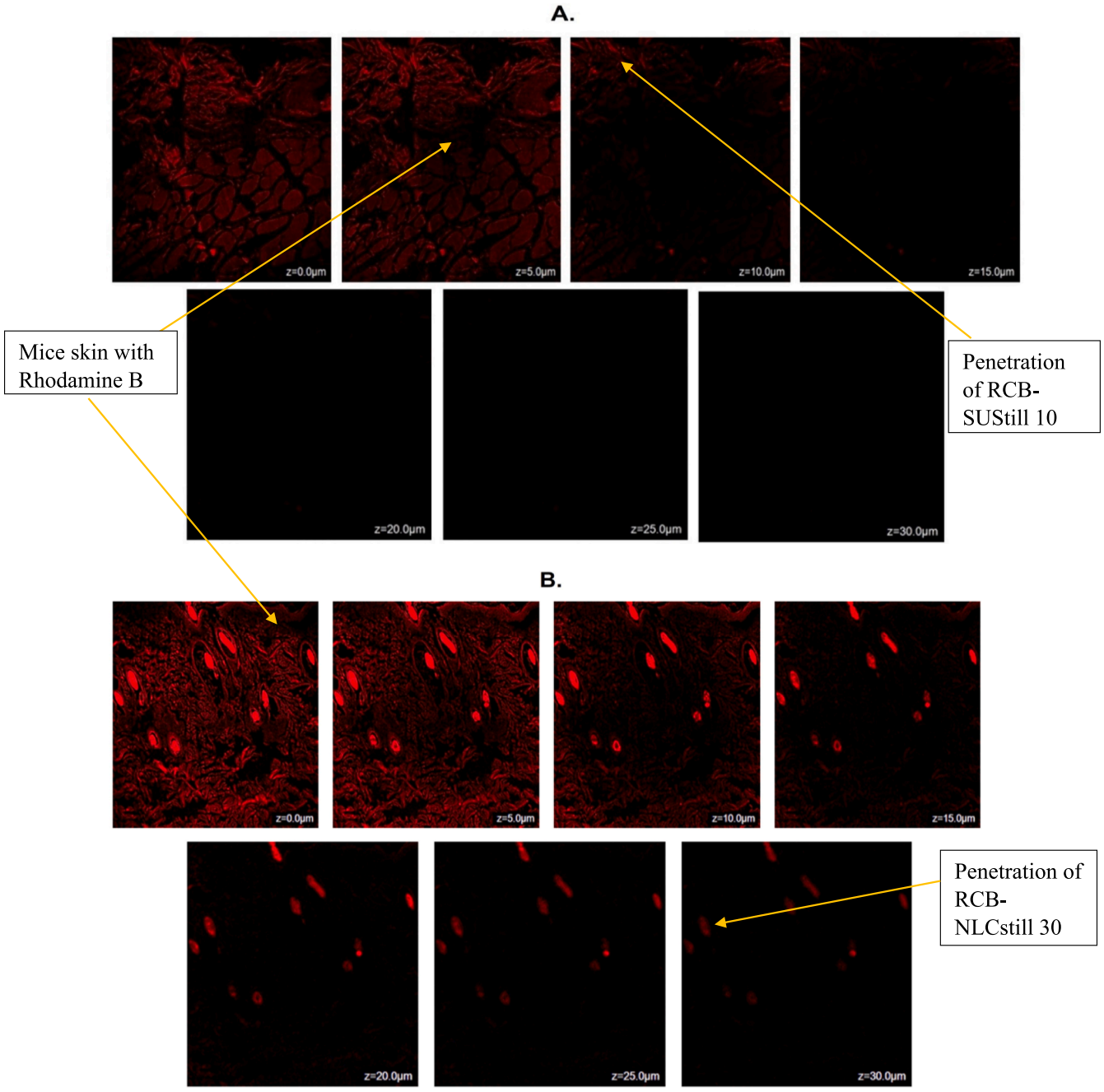

Fig. 10. Confocal laser microscopy of (A) Rhodamine-B-solution with RCB-SUS Gel and (B) Rhodamine-B-loaded RCB-NLCs Gel.

was devoid of aggregation. The RCB-NLCs gel's pH value was observed to be 6.63 ± 0.24, which is harmless and suitable with skin to completely remove the possibility of skin irritation after usage. It was discovered that the drug content of RCB in the RCB-NLCs gel preparation was 97.96 ± 1.25 %, indicating that the content was both within permissible bounds and equally distributed in the preparation.

4.9.2. Viscosity and spreadability

In order to create a consistent, stable, and simple-to-use pharmaceutical composition, the viscosity and spreadability of RCB-NLCs gel were assessed. The RCB-NLCs gel's viscosity was determined to be 9265 ± 42 cP, which reflects the gel's outstanding physical behavior. Maximum viscosity lengthens the gel's stay on the skin's surface, extending the penetration period. Spreadability is a key element of topical preparations from the standpoint of patient compliance. If the base of the formulation distributes readily on the skin, applying it to an irritated region will be more comfortable. The RCB-NLC gel's ultimate diameter was measured to be 7.32 ± 0.25 cm and RCB-SUS gel was 3.87 ± 0.17, indicating spreadability of NLC containing RCB was good as compared to the suspension gel.

4.9.3. Texture analysis of gel

The peak force measurement reflects the formulation's firmness and indicates its gel concentration. The positive area under curve up to this point quantifies consistency, providing insights into the gel's spreadability. The maximum negative force reflects sample cohesiveness, offering insights into how easily the sample can be extruded from a tube. The negative area of curve, referred to as the work of cohesion, signifies both cohesiveness and the formulation's consistency/viscosity. The texture study results explained that the RCB-NLC gel displayed firmness

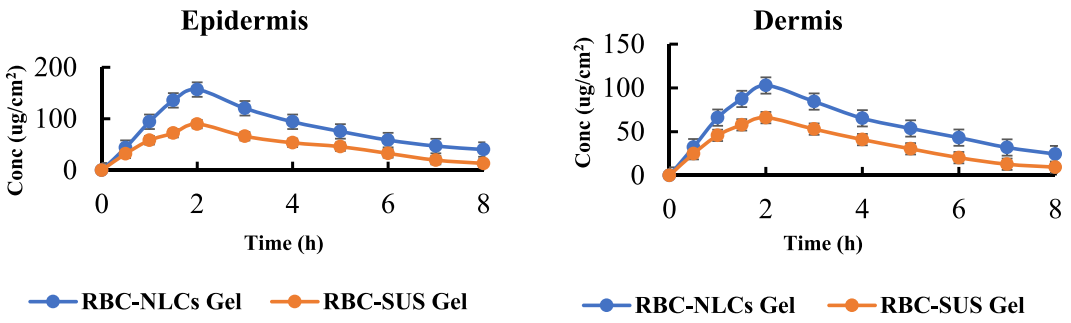

Fig. 11. The variation of RCB concentration on (A) Epidermis and (B) Dermis.

Table 6
Stability testing data.

Test	25 °C/60 % RH			32 °C/60 % RH)			40 °C/75 % RH		
	1	3	6	1	3	6	1	3	6
Colour	Clear								
Homogeneity	Good								
pH	6.64	6.68	6.72	6.64	6.66	6.69	6.68	6.74	6.81
Viscosity	Good								

Table 7
Mice skin exposed to DMBA + 1 % croton oil for the development of skin tumor.

Group	Mean of skin tumor size in mice(mm)			
	0 week	2nd week	4th week	6th week
I. Control	0	0	0	0
II. Carcinogenic control	3	3	3	3
III. Marketed formulation	3	2.41 ± 0.42	1.69 ± 0.28	0.82 ± 0.13
IV. RCB-NLCs gel	3	2.23 ± 0.33	1.36 ± 0.21	0.53 ± 0.10

of 58.87 g, consistency of 503.73 g s, the cohesiveness of −40.86 g and index of the viscosity of −303.01 g s (Fig. 8). A potential explanation could be the existence of excipients in the RCBNLCs preparation. The values discovered above primarily indicate the NLC's capability to be easily employed to the skin in the case of the produced RCB-NLC.

4.9.4. Skin permeation study by ex-vivo

The *ex-vivo* permeation investigation, which used mice skin as a diffusion barrier on the FDC, was employed to establish the permeation of the RCB from NLCs gel and suspensions. This was done to ascertain whether delivery technique was more efficient. The RCB-NLCs showed 82.62 ± 2.08 % permeation in that time frame with flux 2.17 μg/cm^2/hr, in contrast to the RCB-SUS, which showed 43.28 ± 1.84 % penetration after 24 h (Fig. 9). It was discovered that the two variables had a statistically significant association. It was discovered that the release sequence seen during the *in-vitro* permeation investigations and the *in-vitro* research were connected. The RCB-NLCs gel exhibited a 1.91 time higher in drug permeation in comparison to the RCB-SUS gel's drug penetration. This may be due to the RCB-NLCs gel's longer retention time, which contributed to a higher penetration rate and the intended extended release of the drug across skin, acting as a drug reservoir and proving the gel's effectiveness in drug permeation experiments (Qizilbash et al., 2022).

4.10. Determination of depth of permeation by CLSM

According to Fig. 10, the CLSM pictures of mice skin stained with Rhodamine B revealed the depth of RCB-NLC and RCB-SUS penetration after 4 h of dosage administration. For both formulas, the deepness of permeation via the z-axis is 30 μm. Even at 30 μm of depth, the results clearly showed that RCB-NLCs had enhanced fluorescence in contrast to

Table 8
Observations of the study of Lipid Peroxidation Estimation.

Group	Mean of glutathione content (μmol/g protein)		
	0 week(±SD)	3rd weeks (±SD)	6th weeks (±SD)
I. Control	32.76 ± 2.13	32.54 ± 2.22	32.66 ± 2.09
II. Carcinogenic control	387.02 ± 2.42	387.15 ± 7.53	387.09 ± 7.12
III. Marketed formulation	387.89 ± 1.64	209.32 ± 2.18	68.06 ± 1.88
IV. RCB-NLCs gel	387.76 ± 1.08	201.26 ± 2.11	51.84 ± 1.42

RCB-SUS. The finding indicates increased RCB-NLC penetration, which may be related to NLCs' tiny PS and the involvement of lipids and surfactants in enhancing penetration (Soni et al., 2018).

4.11. Dermatokinetic estimation

The concentration of RCB in the dermis and epidermis of mice's skin after the study with RCB-SUS gel and RCB-NLCs gel at specific time difference is depicted in Fig. 11. The dermatokinetic factors are as follows:

For mice skin treated with RCB-SUS gel:

- $C_{Skin\ max}$ value was 89.66 ± 4.85 μg/cm^2 in the epidermis and 66.05 ± 3.54 μg/cm^2 in the dermis.
- $AUC_{0\text{-}t}$ was 372.45 ± 11.58 μg/cm^{2}h in the epidermis and 276.07 ± 9.31 μg/cm^{2}h in the dermis.
- For mice skin treated with RCB-NLCs gel:
- $C_{Skin\ max}$ value was 156.73 ± 7.72 μg/cm^2 in the epidermis and 102.77 ± 6.83 μg/cm^2 in the dermis.
- $AUC_{0\text{-}t}$ was 670.04 ± 13.76 μg/cm^{2}h in the epidermis and 460.78 ± 14.32 μg/cm^{2}h in the dermis.

Notably, a higher amount of RCB was maintained in both the layers of mice's skin when treated with RCB-NLCs gel comparable to the RCB-SUS gel preparation. This can be accredited to the nano-sized vesicle in the formulated formulation, which ease the permeable of vesicles through the skin lipid layers.

Table 9
Skin-irritation score for RCB-NLCs gel.

Formulation code	Group	Score after (day)							Mean score
		1st	2nd	3rd	4th	5th	6th	7th	
Marketed formulation	I	6	6	7	5	6	6	8	6.29
RCB-NLCs gel	II	6	5	6	6	7	6	5	5.86

4.12. Stability study

To ensure the QSE (quality, safety, and efficacy) of the productduring its shelf life, a stability study was conducted in accordance with ICH requirements because it demonstrated superior quality characteristics. The formulation of NLCs exhibited no variations in colour, odor, homogeneity, pH, or viscosity after 1, 3, and 6 months of stability testing (Table 6).

4.13. Assessment of in vivo efficacy

4.13.1. Visual appearance

The findings from visual observations, as presented in Table 7, reveal a consistent decrease in tumor size in groups III (those administered with the commercial formulation) and IV (those treated with the RCB-NLC preparation) during the 2nd and 4th weeks of use. Notably, by the sixth week, the mice treated with the 1 % RCB-NLCs gel demonstrated the most substantial decrease in tumor size in comparison to the marketed formulation.

4.13.2. Biochemical determination

The lipid peroxidation study results highlight the superior effectiveness of the RCB-NLCs gel compared to the marketed product. Specifically, the lipid peroxidation values for the skin treated with RCB-NLCs gel were closer to the values observed in normal skin, as illustrated in Table 8.

4.13.3. Skin irritation study

The mean skin-irritation score for both the RCB-NLCs gel and the commercialized product were calculated to be 5.86 and 6.29, as shown in Table 9. Following the criteria outlined by Uttley & Van Abbe (1973), when these scores fall within the range of 0 to 9, the applied formulation is considered nonirritant to the skin (Uttley and Van Abbe, 1973). This nonirritating nature can be accredited to the encapsulation of RCB within the formulation, as its release primarily targets cancer cells without causing harm or irritation to normal cells.

5. Discussion

RCB-loaded NLCs were prepared with the help of solvent evaporation method, and the preparation was optimized with the help of BBD. The optimized formulation achieved a small PS and low PDI, enhancing its ability to permeate the skin. This optimized formulation displayed controlled release over a 24-hour period. The NLCs gel exhibited enhanced permeable and skin retention. The results indicate that NLCs loaded with RCB have the potential for enhanced topical delivery with improved skin retention. The newly developed formulation underwent extensive characterization, including PS, EE, and zeta potential assessment after optimization by the BBD. The particles were found to have a spherical shape, and the entrapment efficiency was satisfactory. *In vitro* release studies demonstrated that the NLCs were able of controlled release of RCB for up to 24 h (Sartaj and Annu, 2022). In comparison to a conventional gel formulation, ex-vivo studies showed a significant 1.91-fold increase in the skin's ability to retain the substance. As per the CLSM finding indicates increased RCB-NLC penetration, which may be related to NLCs' small PS and the involvement of lipids and surfactants in enhancing penetration (Soni et al., 2018). Dermatokinetic study: Notably, a higher amount of RCB was maintained in both the layers of mice's skin when treated with RCB-NLCs gel comparable to the RCB-SUS gel preparation. The formulation of NLCs exhibited no variations in colour, odor, homogeneity, pH, or viscosity after 1, 3, and 6 months of stability testing. In the in-vivo study, the findings from visual observations, as presented in Table 6, reveal a consistent decrease in tumor size in groups III (those administered with the commercial formulation) and IV (those treated with the RCB-NLC preparation) during the 2nd and 4th weeks of use. Notably, by the sixth week, the mice treated with the 1 % RCB-NLCs gel demonstrated the most substantial decrease in tumor size in comparison to the marketed formulation. The lipid peroxidation study results highlight the superior effectiveness of the RCB-NLCs gel compared to the marketed product. The mean skin-irritation score for both the RCB-NLCs gel and the commercialized product were calculated to be 5.86 and 6.29. Following the criteria outlined when these scores fall within the range of 0 to 9, the applied formulation is considered nonirritant to the skin.

6. Conclusion

We have successfully formulated and assessed RCB-NLCs is a capable for the management of skin cancer. The prepared NLCs were fine-tuned with a focus on PS, PDI, zeta potential, and EE. *In vitro* release studies demonstrated that the NLCs were able of controlled release of RCB for up to 24 h. In comparison to a conventional gel formulation, ex-vivo studies showed a significant increase in the skin's ability to retain the substance. The optimized NLCs enhanced the release characteristics of RCB and demonstrated favorable outcomes in both in-vivo and biochemical investigations. Based on the collective results, the encapsulation of RCB within NLCs emerges as a promising strategy for the management of skin cancer.

Declaration of competing interest

The authors declare that they have no known competing financial interests or personal relationships that could have appeared to influence the work reported in this paper.

Acknowledgement

This project was supported by the Scientific Research Center at Buraydah Private Colleges under the research project # BPC-SRC/2022-005.

References

Afaq, F., 2011. Natural agents: Cellular and molecular mechanisms of photoprotection. Arch. Biochem. Biophys. 508, 144–151. https://doi.org/10.1016/J.ABB.2010.12.007.

Ahmed, M.M., Fatima, F., Alali, A., Kalam, M.A., Alhazzani, K., Bhatia, S., Alshehri, S., Ghoneim, M.M., 2022. Ribociclib-loaded ethylcellulose-based nanosponges: formulation, physicochemical characterization, and cytotoxic potential against breast cancer. Adsorp. Sci. Tech., 1922263 https://doi.org/10.1155/2022/1922263.

Alam, T., Khan, S., Gaba, B., Haider, M.F., Baboota, S., Ali, J., 2018. Adaptation of quality by design-based development of isradipine nanostructured-lipid carrier and its evaluation for in vitro gut permeation and in vivo solubilization fate. J. Pharm. Sci. 107, 2914–2926. https://doi.org/10.1016/j.xphs.2018.07.021.

Alam, M., Rizwanullah, M., Mir, S.R., Amin, S., 2023. Statistically optimized tacrolimus and thymoquinone co-loaded nanostructured lipid carriers gel for improved topical treatment of psoriasis. Gels 9, 515. https://doi.org/10.3390/GELS9070515.

Alhalmi, A., Amin, S., Khan, Z., Beg, S., Al Kamaly, O., Saleh, A., Kohli, K., 2022. Nanostructured lipid carrier-based codelivery of raloxifene and naringin: formulation, optimization, in vitro, ex vivo, in vivo assessment, and acute toxicity studies. Pharmaceutics 14, 1771. https://doi.org/10.3390/PHARMACEUTICS14091771/S1.

Al-Shdefat, R., Hailat, M., Alshogran, O.Y., Abu Dayyih, W., Gardouh, A., Al Meanazel, O., 2023. Ribociclib hybrid lipid-polymer nanoparticle preparation and characterization for cancer treatment. Polymers 15, 2844. https://doi.org/10.3390/polym15132844.

Apalla, Z., Lallas, A., Sotiriou, E., Lazaridou, E., Ioannides, D., 2017. Epidemiological trends in skin cancer. Dermatol. Pract. Concept. 7, 1. https://doi.org/10.5826/DPC.0702A01.

(ASCO) ASoCO, 2021. Skin Cancer (Non-Melanoma): StatisticsCancer Facts & Figures.

Aziz, K., Ahmad, N., Kohli, K., 2017. Enhanced anti arthritic potential of tacrolimus by transdermal nanocarrier system. J. Nanosci. Nanotechnol. 17, 4573–4583. https://doi.org/10.1166/JNN.2017.14108.

Batool, S., Sohail, S., ud Din, F., Alamri, A.H., Alqahtani, A.S., Alshahrani, M.A., Alshehri, M.A., Choi, H.G., 2023. A detailed insight of the tumor targeting using nanocarrier drug delivery system. Drug Deliv. 30 (1), 2183815.

Burris, H.A., 2018. Ribociclib for the treatment of hormone receptor-positive, human epidermal growth factor receptor 2-negative advanced breast cancer. Expert Rev. Anticancer Ther. 18, 201–213. https://doi.org/10.1080/14737140.2018.1435275.

Chaudhary, S.C., Alam, M.S., Siddiqui, M.S., Athar, M., 2009. Chemopreventive effect of farnesol on DMBA/TPA-induced skin tumorigenesis: involvement of inflammation, Ras-ERK pathway and apoptosis. Life Sci. 85, 196–205. https://doi.org/10.1016/j.lfs.2009.05.008.

Cohen, J.L., 2010. Actinic keratosis treatment as a key component of preventive strategies for nonmelanoma skin cancer. J. Clin. Aesthetic Dermatol. 3, 39–44.

Danaei, M., Dehghankhold, M., Ataei, S., Hasanzadeh Davarani, F., Javanmard, R., Dokhani, A., Khorasani, S., Mozafari, M.R., 2018. Impact of particle size and polydispersity index on the clinical applications of lipidic nanocarrier systems. Pharmaceutics 10 (2), 57.

Das, R.K., Hossain, S.K.U., Bhattacharya, S., 2005. Diphenylmethyl selenocyanate inhibits DMBA-croton oil induced two-stage mouse skin carcinogenesis by inducing apoptosis and inhibiting cutaneous cell proliferation. Cancer Lett. 230, 90–101. https://doi.org/10.1016/j.canlet.2004.12.021.

Doran, C.M., Ling, R., Byrnes, J., Crane, M., Shakeshaft, A.P., Searles, A., Perez, D., 2016. Benefit cost analysis of three skin cancer public education mass-media campaigns implemented in new south wales, Australia. Plos One 11, e0147665. https://doi.org/10.1371/JOURNAL.PONE.0147665.

El-Housiny, S., Eldeen, M.A.S., El-Attar, Y.A., Salem, H.A., Attia, D., Bendas, E.R., El-Nabarawi, M.A., 2018. Fluconazole-loaded solid lipid nanoparticles topical gel for treatment of pityriasis versicolor: formulation and clinical study. Drug Deliv. 25, 78–90. https://doi.org/10.1080/10717544.2017.1413444.

Fei, Z., Yoosefian, M., 2021. Design and development of polymeric micelles as nanocarriers for anti-cancer Ribociclib drug. J. Mol. Liq. 329, 115574 https://doi.org/10.1016/j.molliq.2021.115574.

Garaga, M.N., Jayakody, N., Fraenza, C.C., Itin, B., Greenbaum, S., 2021. Molecular-level insights into structure and dynamics in ionic liquids and polymer gel electrolytes. J. Mol. Liq. 329, 115454 https://doi.org/10.1016/j.molliq.2021.115454.

Ghazwani, M., Hani, U., Alqarni, M.H., Alam, A., 2023. Beta caryophyllene-loaded nanostructured lipid carriers for topical management of skin disorders: statistical optimization, in vitro and dermatokinetic evaluation. Gels 9 (7), 550.

González-Mira, E., Nikolić, S., García, M.L., Egea, M.A., Souto, E.B., Calpena, A.C., 2011. Potential use of nanostructured lipid carriers for topical delivery of flurbiprofen. J. Pharm. Sci. 100, 242–251. https://doi.org/10.1002/jps.22271.

Gupta, D.K., Aqil, M., Ahad, A., Imam, S.S., Waheed, A., Qadir, A., Iqubal, M.K., Sultana, Y., 2020. Tailoring of berberine loaded transniosomes for the management of skin cancer in mice. J. Drug Deliv. Sci. Technol. 60, 102051 https://doi.org/10.1016/j.jddst.2020.102051.

Harde, H., Agrawal, A.K., Katariya, M., Kale, D., Jain, S., 2015. Development of a topical adapalene-solid lipid nanoparticle loaded gel with enhanced efficacy and improved skin tolerability. RSC Adv. 5, 43917–43929. https://doi.org/10.1039/C5RA06047H.

Hennings, H., Devor, D., Wenk, M.L., Slaga, T.J., Former, B., Colburn, N.H., Bowden, G. T., Elgjo, K., Yuspa, S.H., 1981. Comparison of Two-Stage Epidermal Carcinogenesis Initiated by 7,12-Dimethylbenz(a)anthracene or A/-Methyl-A/'-nitro-A/-nitrosoguamdine in Newborn and Adult SENCAR and BALB/c Mice. Cancer Res. 41, 773–779.

Infante, J.R., Cassier, P.A., Gerecitano, J.F., Witteveen, P.O., Chugh, R., Ribrag, V., Chakraborty, A., Matano, A., Dobson, J.R., Crystal, A.S., Parasuraman, S., Shapiro, G.I., 2016. A phase i study of the cyclin-dependent kinase 4/6 inhibitor ribociclib (LEE011) in patients with advanced solid tumors and lymphomas. Clin. Cancer Res. 22, 5696–5705. https://doi.org/10.1158/1078-0432.CCR-16-1248/274394/AM/A-PHASE-I-STUDY-OF-THE-CYCLIN-DEPENDENT-KINASE-4-6.

Iqbal, B., Ali, J., Baboota, S., 2018. Silymarin loaded nanostructured lipid carrier: From design and dermatokinetic study to mechanistic analysis of epidermal drug deposition enhancement. J. Mol. Liq. 255, 513–529. https://doi.org/10.1016/j.molliq.2018.01.141.

Iqubal, M.K., Iqubal, A., Imtiyaz, K., Rizvi, M.M.A., Gupta, M.M., Ali, J., Baboota, S., 2021. Combinatorial lipid-nanosystem for dermal delivery of 5-fluorouracil and resveratrol against skin cancer: Delineation of improved dermatokinetics and epidermal drug deposition enhancement analysis. Eur. J. Pharm. Biopharm. 163, 223–239. https://doi.org/10.1016/j.ejpb.2021.04.007.

Jenning, V., Thünemann, A.F., Gohla, S.H., 2000. Characterisation of a novel solid lipid nanoparticle carrier system based on binary mixtures of liquid and solid lipids. Int. J. Pharm. 199, 167–177. https://doi.org/10.1016/S0378-5173(00)00378-1.

Khan, A.A., Mudassir, J., Akhtar, S., Murugaiyah, V., Darwis, Y., 2019. Freeze-Dried Lopinavir-loaded nanostructured lipid carriers for enhanced cellular uptake and bioavailability: statistical optimization, in vitro and in vivo evaluations. Pharmaceutics 11, 97. https://doi.org/10.3390/PHARMACEUTICS11020097.

Khan, S., Shaharyar, M., Fazil, M., Baboota, S., Ali, J., 2016. Tacrolimus-loaded nanostructured lipid carriers for oral delivery – Optimization of production and characterization. Eur. J. Pharm. Biopharm. 108, 277–288. https://doi.org/10.1016/j.ejpb.2016.07.017.

Kumar, P., Sharma, G., Kumar, R., Malik, R., Singh, B., Katare, O.P., Raza, K., 2017. Enhanced brain delivery of dimethyl fumarate employing tocopherol-acetate-based nanolipidic carriers: evidence from pharmacokinetic, biodistribution, and cellular uptake studies. ACS Chem. Neurosci. 8, 860–865. https://doi.org/10.1021/acschemneuro.6b00428.

Leiter, U., Eigentler, T., Garbe, C., 2014. Epidemiology of Skin Cancer. Sunlight, Vitam. D Ski. Cancer 120–140. https://doi.org/10.1007/978-1-4939-0437-2_7.

Luo, Q., Zhao, J., Zhang, X., Pan, W., 2011. Nanostructured lipid carrier (NLC) coated with Chitosan Oligosaccharides and its potential use in ocular drug delivery system. Int. J. Pharm. 403, 185–191. https://doi.org/10.1016/j.ijpharm.2010.10.013.

Malik, M., Ali, Z., Khan, S., Zeb, A., ud Din, F., Almari, A., Lahiq, A.A., 2023. TPGS-PLA nanomicelles for targeting lung cancer; synthesis, characterization, and in vitro antitumor efficacy. J. Drug Deliv. Sci. Technol. 3, 105238.

Moolakkadath, T., Aqil, M., Ahad, A., Imam, S.S., Iqbal, B., Sultana, Y., Mujeeb, M., Iqbal, Z., 2018. Development of transethosomes formulation for dermal fisetin delivery: Box-Behnken design, optimization, in vitro skin penetration, vesicles–skin interaction and dermatokinetic studies. Artif. Cells Nanomed. Biotechnol. 46, 755–765. https://doi.org/10.1080/21691401.2018.1469025.

Nabi, B., Rehman, S., Aggarwal, S., Baboota, S., Ali, J., 2020. Quality by design adapted chemically engineered lipid architectonics for HIV therapeutics and intervention: contriving of formulation, appraising the in vitro parameters and in vivo solubilization potential. AAPS PharmSciTech 21, 1–17. https://doi.org/10.1208/S12249-020-01795-W/METRICS.

Nair, A., Jacob, S., Al-Dhubiab, B., Attimarad, M., Harsha, S., 2013. Basic considerations in the dermatokinetics of topical formulations. Brazilian J. Pharm. Sci. 49, 423–434. https://doi.org/10.1590/S1984-82502013000300004.

Negi, L.M., Talegaonkar, S., Jaggi, M., Verma, A.K., Verma, R., Dobhal, S., Kumar, V., 2014. Surface engineered nanostructured lipid carriers for targeting MDR tumor: Part II. In vivo biodistribution, pharmacodynamic and hematological toxicity studies. Colloids Surf. B Biointerfaces 123, 610–615. https://doi.org/10.1016/j.colsurfb.2014.09.061.

Negi, L.M., Jaggi, M., Joshi, V., Ronodip, K., Talegaonkar, S., 2015. Hyaluronic acid decorated lipid nanocarrier for MDR modulation and CD-44 targeting in colon adenocarcinoma. Int. J. Biol. Macromol. 72, 569–574. https://doi.org/10.1016/j.ijbiomac.2014.09.005.

Ohkawa, H., Ohishi, N., Yagi, K., 1979. Assay for lipid peroxides in animal tissues by thiobarbituric acid reaction. Anal. Biochem. 95, 351–358. https://doi.org/10.1016/0003-2697(79)90738-3.

Perera, E., Gnaneswaran, N., Staines, C., Win, A.K., Sinclair, R., 2015. Incidence and prevalence of non-melanoma skin cancer in Australia: a systematic review. Australas. J. Dermatol. 56, 258–267. https://doi.org/10.1111/AJD.12282.

Qizilbash, F.F., Ashhar, M.U., Zafar, A., Qamar, Z., Annu, A.J., Baboota, S., Ghoneim, M. M., Alshehri, S., Ali, A., 2022. Thymoquinone-enriched naringenin-loaded nanostructured lipid carrier for brain delivery via nasal route: in vitro prospect and in vivo therapeutic efficacy for the treatment of depression. Pharmaceutics 14, 656. https://doi.org/10.3390/pharmaceutics14030656.

Raza, K., Singh, B., Lohan, S., Sharma, G., Negi, P., Yachha, Y., Katare, O.P., 2013. Nano-lipoidal carriers of tretinoin with enhanced percutaneous absorption, photostability, biocompatibility and anti-psoriatic activity. Int. J. Pharm. 456, 65–72. https://doi.org/10.1016/j.ijpharm.2013.08.019.

Rizwanullah, M., Perwez, A., Mir, S.R., Rizvi, M.M.A., Amin, S., 2021. Exemestane encapsulated polymer-lipid hybrid nanoparticles for improved efficacy against breast cancer: optimization, in vitro characterization and cell culture studies. Nanotechnology 32, 415101. https://doi.org/10.1088/1361-6528/AC1098.

Sartaj, A., Annu, Biswas, L., Verma, A.K., Sahoo, P.K., Baboota, S., Ali, J., 2022. Ribociclib Nanostructured Lipid Carrier Aimed for Breast Cancer: Formulation Optimization, Attenuating In Vitro Specification, and In Vivo Scrutinization. Biomed Res. Int. 2022, Article ID 6009309 (Pages-24). https://doi.org/10.1155/2022/6009309.

Shah, K.A., Date, A.A., Joshi, M.D., Patravale, V.B., 2007. Solid lipid nanoparticles (SLN) of tretinoin: Potential in topical delivery. Int. J. Pharm. 345, 163–171. https://doi.org/10.1016/j.ijpharm.2007.05.061.

Sharma, M., Mittapelly, N., Banala, V.T., Urandur, S., Gautam, S., Marwaha, D., Rai, N., Singh, N., Gupta, A., Mitra, K., Mishra, P.R., 2022. Amalgamated microneedle array bearing ribociclib-loaded transfersomes eradicates breast cancer via CD44 targeting. Biomacromol. 23, 661–675. https://doi.org/10.1021/acs.biomac.1c01076.

Shtay, R., Tan, C.P., Schwarz, K., 2018. Development and characterization of solid lipid nanoparticles (SLNs) made of cocoa butter: a factorial design study. J. Food Eng. 231, 30–41. https://doi.org/10.1016/j.jfoodeng.2018.03.006.

Singh, A., Neupane, Y.R., Mangla, B., Kohli, K., 2019. Nanostructured lipid carriers for oral bioavailability enhancement of exemestane: formulation design, in vitro, ex vivo, and in vivo studies. J. Pharm. Sci. 108, 3382–3395. https://doi.org/10.1016/j.xphs.2019.06.003.

Soni, K., Rizwanullah, M., Kohli, K., 2018. Development and optimization of sulforaphane-loaded nanostructured lipid carriers by the Box-Behnken design for improved oral efficacy against cancer: in vitro, ex vivo and in vivo assessments. Artif. Cells, Nanomed. Biotechnol. 46, 15–31. https://doi.org/10.1080/21691401.2017.1408124.

Subedi, R.K., Kang, K.W., Choi, H.K., 2009. Preparation and characterization of solid lipid nanoparticles loaded with doxorubicin. Eur. J. Pharm. Sci. 37, 508–513. https://doi.org/10.1016/j.ejps.2009.04.008.

Teng, Z., Yu, M., Ding, Y., Zhang, H., Shen, Y., Jiang, M., Liu, P., Opoku-Damoah, Y., Webster, T.J., Zhou, J., 2019. Preparation and characterization of nimodipine-loaded nanostructured lipid systems for enhanced solubility and bioavailability. Int. J. Nanomedicine 14, 119–133. https://doi.org/10.2147/IJN.S186899.

Thomas, S.M., Lefevre, J.G., Baxter, G., Hamilton, N.A., 2021 Feb. Interpretable deep learning systems for multi-class segmentation and classification of non-melanoma skin cancer. Med. Image Anal. 1 (68), 101915.

Thotakura, N., Kumar, P., Wadhwa, S., Raza, K., Katare, P., 2017. Dermatokinetics as an important tool to assess the bioavailability of drugs by topical nanocarriers. Curr. Drug Metab. 18, 404–411.

Thuy, V.N., Van, T.V., Dao, A.H., Lee, B.J., 2022. Nanostructured lipid carriers and their potential applications for versatile drug delivery via oral administration. OpenNano 8, 100064. https://doi.org/10.1016/j.onano.2022.100064.

Uttley, M., Van Abbe, N.J., 1973. Primary irritation of the skin: mouse ear test and human patch test procedures. J. SOC. COSMET. Chem. 24, 217–227.

Varshosaz, J., Davoudi, M.A., Rasoul-Amini, S., 2018. Docetaxel-loaded nanostructured lipid carriers functionalized with trastuzumab (Herceptin) for HER2-positive breast cancer cells. J. Liposome Res. 28, 285–295. https://doi.org/10.1080/08982104.2017.1370471.

Waghule, T., Rapalli, V.K., Singhvi, G., Gorantla, S., Khosa, A., Dubey, S.K., Saha, R.N., 2021. Design of temozolomide-loaded proliposomes and lipid crystal nanoparticles with industrial feasible approaches: comparative assessment of drug loading, entrapment efficiency, and stability at plasma pH. J. Liposome Res. 31, 158–168. https://doi.org/10.1080/08982104.2020.1748648.

Xing, R., Mustapha, O., Ali, T., Rehman, M., Zaidi, S.S., Baseer, A., Batool, S., Mukhtiar, M., Shafique, S., Malik, M., Sohail, S., 2021. Development, characterization, and evaluation of SLN-loaded thermoresponsive hydrogel system of topotecan as biological macromolecule for colorectal delivery. BioMed Res. Int.. 3 (2021), 1–4.

Yagi, K., 1987. Lipid peroxides and human diseases. Chem. Phys. Lipids 45, 337–351. https://doi.org/10.1016/0009-3084(87)90071-5.